

miR-153 Regulates SNAP-25, Synaptic Transmission, and Neuronal Development

Chunyao Wei¹*, Elizabeth J. Thatcher¹*, Abigail F. Olena¹, Diana J. Cha¹, Ana L. Perdigoto², Andrew F. Marshall¹, Bruce D. Carter², Kendal Broadie¹, James G. Patton¹*

1 Department of Biological Sciences, Vanderbilt University and Medical School, Nashville, Tennessee, United States of America, **2** Department of Biochemistry, Vanderbilt University and Medical School, Nashville, Tennessee, United States of America

Abstract

SNAP-25 is a core component of the trimeric SNARE complex mediating vesicle exocytosis during membrane addition for neuronal growth, neuropeptide/growth factor secretion, and neurotransmitter release during synaptic transmission. Here, we report a novel microRNA mechanism of SNAP-25 regulation controlling motor neuron development, neurosecretion, synaptic activity, and movement in zebrafish. Loss of *miR-153* causes overexpression of SNAP-25 and consequent hyperactive movement in early zebrafish embryos. Conversely, overexpression of *miR-153* causes SNAP-25 down regulation resulting in near complete paralysis, mimicking the effects of treatment with Botulinum neurotoxin. *miR-153*-dependent changes in synaptic activity at the neuromuscular junction are consistent with the observed movement defects. Underlying the movement defects, perturbation of *miR-153* function causes dramatic developmental changes in motor neuron patterning and branching. Together, our results indicate that precise control of SNAP-25 expression by *miR-153* is critically important for proper neuronal patterning as well as neurotransmission.

Citation: Wei C, Thatcher EJ, Olena AF, Cha DJ, Perdigoto AL, et al. (2013) *miR-153* Regulates SNAP-25, Synaptic Transmission, and Neuronal Development. PLoS ONE 8(2): e57080. doi:10.1371/journal.pone.0057080

Editor: Erik C. Johnson, Wake Forest University, United States of America

Received: December 1, 2012; **Accepted:** January 16, 2013; **Published:** February 25, 2013

Copyright: © 2013 Wei et al. This is an open-access article distributed under the terms of the Creative Commons Attribution License, which permits unrestricted use, distribution, and reproduction in any medium, provided the original author and source are credited.

Funding: This work was supported by grants from the National Institutes of Health (NIH) to JGP (GM 075790 and EY019759), KB (GM 54544), and BDC (NS038220) and by training fellowships to EJT (T32 GM08556) and ALP (F30 NS061403 and T32 GM07347). Antibodies were obtained from the Zebrafish International Resource Center NIH-NCRR, grant RR12546. The funders had no role in study design, data collection and analysis, decision to publish, or preparation of the manuscript.

Competing Interests: The authors have declared that no competing interests exist.

* E-mail: James.G.Patton@Vanderbilt.edu

These authors contributed equally to this work.

Introduction

Trimeric soluble N-ethylmaleimide-sensitive factor attachment protein receptor (SNARE) complexes form the core machinery mediating vesicular exocytosis [1–3]. In the nervous system, SNARE complexes are involved in membrane addition during neuronal growth as well as both dense core vesicle (DCV) release of proteins and synaptic vesicle (SV) release of fast neurotransmitters. At synapses, the core SNARE protein SNAP-25 interacts with accessory proteins that together regulate SV exocytosis by linking Ca²⁺ sensing to membrane fusion and neurotransmitter release [4–7]. SNAP-25 is a specific target of Botulinum neurotoxin proteases that block vesicle release, resulting in rapid paralysis and death [8,9]. Misregulation of SNAP-25 is associated with several human diseases and neurodegenerative disorders including Huntington's Disease [10], Alzheimer's Disease [11], and diabetes [12].

SNAP-25 is required for action potential-evoked glutamatergic, cholinergic, and glycinergic transmission in neurons [13,14]. Mouse knockouts of SNAP-25 are therefore lethal although neuronal cultures from SNAP-25 null mutants maintain the ability to exhibit stimulus-independent transmitter release [13,15]. GABAergic inhibitory synapses express lower levels of SNAP-25 and may be more sensitive to calcium regulation, whereas glutamatergic excitatory synapses express higher amounts of SNAP-25 that alters calcium sensitivity [4]. Part of this differential

regulation could be due to accessory proteins that control SNAP-25 distribution and levels to modulate synaptic activity [16–18]. Transcriptional mechanisms regulating SNAP-25 levels have also been suggested to play key roles in the dynamic control of synaptic function [19–23].

Several miRNAs have been shown to regulate synapse formation or homeostasis, mostly within the post-synaptic dendrite [22,24,25]. On the presynaptic side, most forms of regulation center on modulation of calcium channels and calcium-dependent vesicle release [26,27]. In this study, we show that *miR-153* inhibits SNAP-25 expression in the developing nervous system. Precise control of SNAP-25 by *miR-153* is necessary not only for presynaptic vesicle release, but also for protein secretion, motor neuron patterning, and outgrowth.

Results

miR-153 Regulates Embryonic Movement

miR-153 has been proposed to be one of a limited number of ancient miRNAs that evolved with the establishment of tissue identity [28]. It is conserved among bilaterians displaying distinct expression patterns in neurosecretory brain cells of the deuterostome marine worm *Platynereis dumerilii* and the protostome annelid *Capitella* [28]. In zebrafish, *miR-153* is expressed in distinct regions of the developing nervous system and brain, including neurose-

cretory cells of the hypothalamus [29,30]. Using deep sequencing and *in situ* localization, we detected robust *miR-153* expression in the developing zebrafish brain and reduced, but detectable levels in the spinal cord as early as the 18 somite stage, with progressively increasing expression thereafter [30,31] [32].

To determine the function of *miR-153*, we injected either synthetic *miR-153* or antisense morpholinos against *miR-153* into single cell embryos and allowed development to proceed for 1–2 days. Two different morpholinos were used to ensure specificity and we verified overexpression and knockdown of *miR-153* using northern blots (Fig. S1). No gross morphological changes were observed in injected embryos and normal localization of neuronal markers was detected at the midbrain-hindbrain boundary, inner ear, and retina at 1–2 dpf (data not shown). Despite the lack of morphological changes, we observed striking behavioral movement defects in injected embryos. To quantify movement, embryos were recorded over time (Movie S1) with analyses restricted to embryos within the chorion at 24 hpf. Normal zebrafish embryos move within the chorion with a characteristic frequency of ~ 1 twitch/minute at 24 hpf (Fig. 1). Strikingly, embryos injected with *miR-153* were almost completely motionless, with little or no spontaneous movement, although their hearts were beating normally and minimal movement could be elicited by touch stimulation (Fig. 1). In contrast, knockdown of *miR-153* caused a dramatic and significant 7-fold increase in the frequency of spontaneous movement (Fig. 1). Interestingly, upon touch stimulation, *miR-153* morphants would initially respond with unusually robust, hyperactive movements after which all motion would cease altogether for a period of time (whether touched or not), followed by a resumption of hyperactive movement upon stimulation. At 52 hpf, *miR-153* overexpression fish embryos were still mostly motionless, while *miR-153* knockdown embryos were still hyperactive (data not shown).

miR-153 Targets *snap-25*

To identify mRNAs regulated by *miR-153*, we used target prediction algorithms, compared the expression patterns of both potential mRNA targets and *miR-153*, and assayed phenotypes from gain and loss of function experiments. Based on these criteria, *snap-25* proved to be a *bona fide* target for *miR-153* based on the results of reporter silencing experiments (Fig. 2) and consistent with conservation of miRNA recognition elements (MREs) from fish to humans (Fig. S2).

There are two SNAP-25 paralogs in zebrafish (*a* and *b* isoforms) with similar, but not identical, 3' UTRs [33,34]. For reporter assays, we fused the 3' UTR from both *snap-25* isoforms to the GFP reading frame (*snap-25a* data shown in Fig. 2A; *snap-25b* shown in Fig. S3). Synthetic mRNAs prepared from these reporters were injected into single cell embryos in the presence or absence of exogenous *miR-153* or *miR-153* morpholinos (MOs). Based on fluorescence levels in live embryos at 1 dpf, co-injection of *miR-153* resulted in obvious down-regulation of GFP for both isoforms (Fig. 2B). To confirm that the loss of GFP was due to pairing with the predicted MREs, we created deletions of individual and combinations of MREs in *snap-25a* and *snap-25b*. Deletion of both MREs from *snap-25a* and all three MREs from *snap-25b* abolished the ability of *miR-153* to silence expression (Fig. 2B; Fig. S3B). For *snap-25a*, we tested each of the individual MREs and found that deletion of a single MRE resulted in only modest silencing whereas deletion of both MREs caused a loss of silencing. We conclude that *miR-153* targets both isoforms of *snap-25* in an MRE-dependent manner.

If *miR-153* targets *snap-25*, knockdown of endogenous *miR-153* should lead to increased reporter fluorescence. To test this prediction, antisense morpholinos were co-injected with reporter mRNAs (Fig. 2). We found that knockdown of *miR-153* caused a significant increase in GFP expression compared to embryos with wild type levels of endogenous *miR-153*. Lastly, we performed western blots using antibodies against GFP and analyzed protein

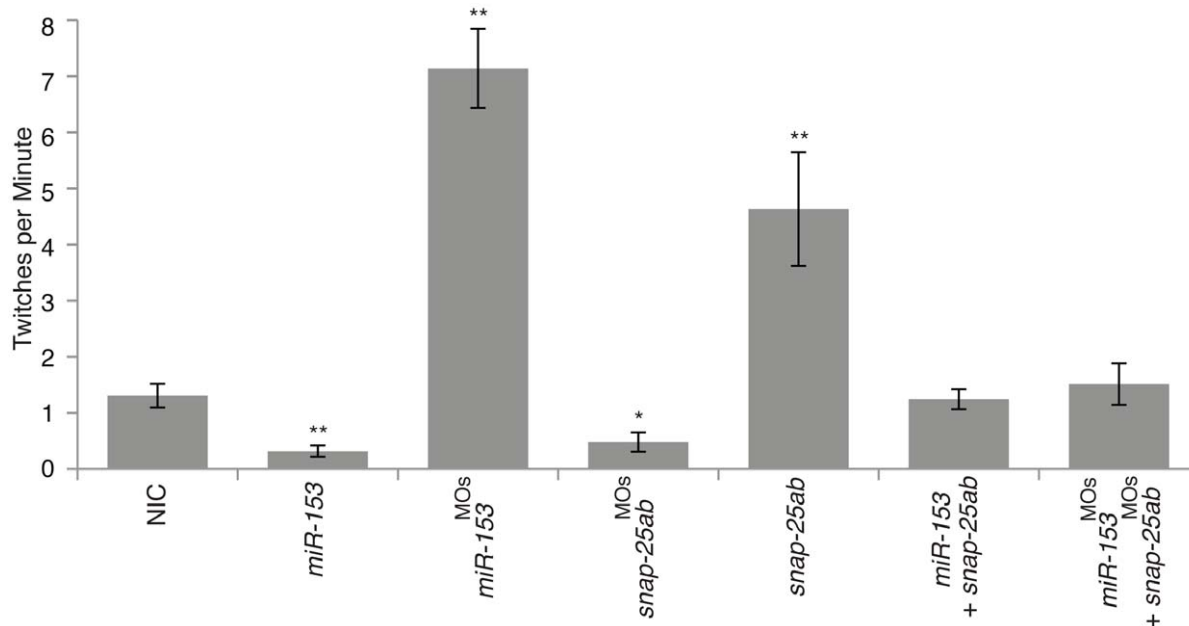


Figure 1. *miR-153* regulates embryonic movement. Embryonic movement was recorded at 1 dpf for each of the singly and multiple injected conditions shown (see Movies). The number of twitches per minute was counted and significance determined by comparing the noninjected control (NIC) embryos to all other conditions using ANOVA with Dunnett's post-test. *, $p < 0.05$; **, $p < 0.01$. Movements were counted for approximately 60 embryos over 2–5 minutes for each condition. doi:10.1371/journal.pone.0057080.g001

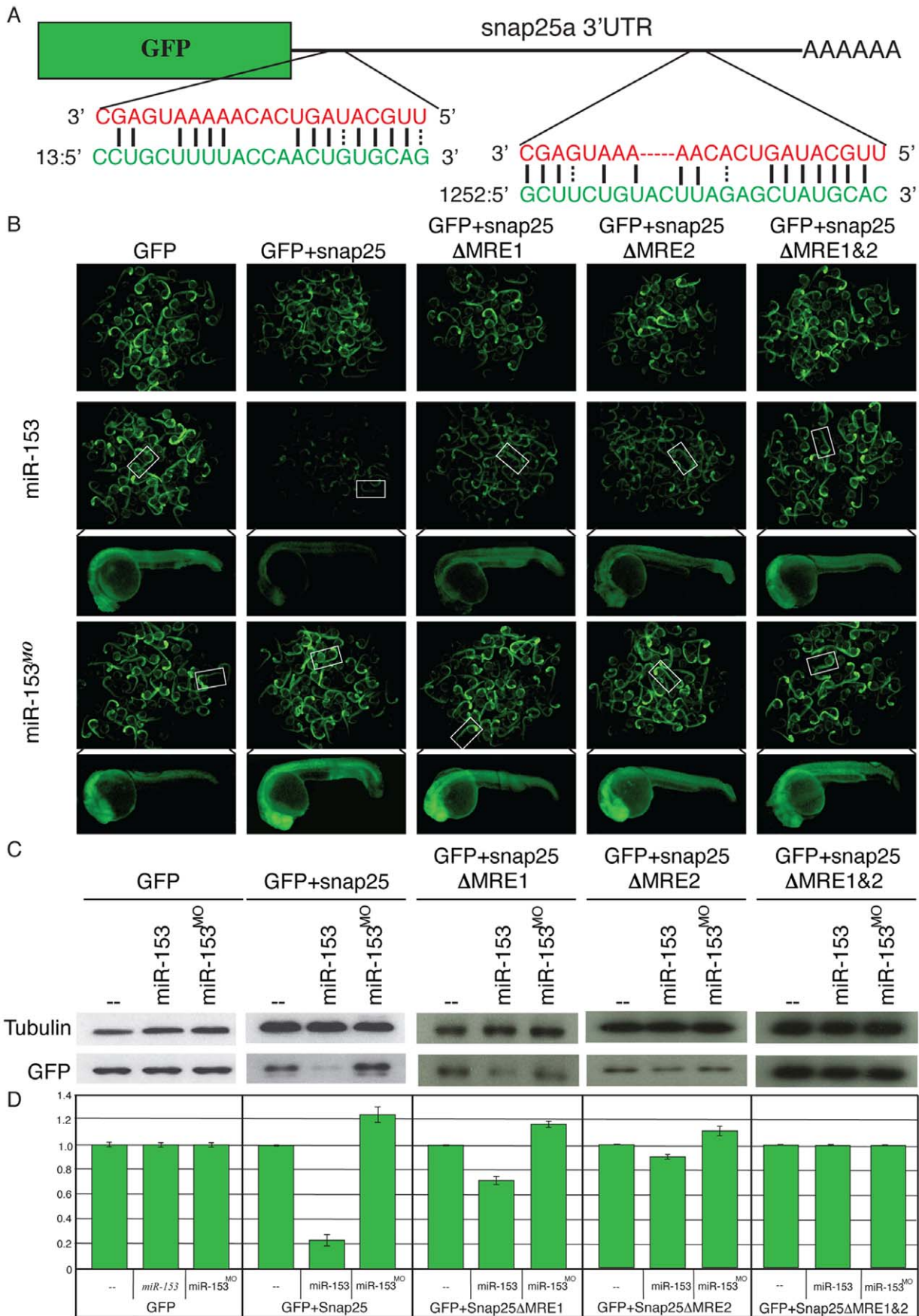


Figure 2. miR-153 targets snap-25a. (A) GFP reporter constructs were created by fusing the reading frame of GFP to the *snap-25a* 3' UTR. Two predicted miRNA recognition elements (MREs) were identified in the *snap-25a* 3' UTR. The *miR-153* sequence is indicated in red and the corresponding *snap-25a* UTR sequence is shown in green. (B) Single cell zebrafish embryos were injected with mRNAs derived from GFP reporters lacking a UTR (GFP), fused to the full length *snap-25a* UTR (+*snap-25*), or mutant versions of the *snap-25a* UTR lacking individual MREs (*snap-25a*ΔMRE1 and *snap-25a*ΔMRE2) or both MREs (*snap-25a*ΔMRE1&2). Embryos were injected in the presence or absence of exogenous *miR-153* or morpholinos against *miR-153* (*miR-153*^{MO}). Fluorescence levels were examined at 1 dpf. Clusters of embryos (~60) are shown as well as a high magnification image of a single representative embryo. (C) Lysates from ~100 embryos were prepared from embryos treated as in B and GFP protein levels were determined by western blotting using antibodies against GFP or control antibodies against α -tubulin. (D) Quantitation of westerns was performed with a paired Student's t-test (n = 5). doi:10.1371/journal.pone.0057080.g002

levels in lysates prepared from pools of embryos treated as above (Fig. 2C,D). The levels of GFP mirrored the effects observed using fluorescence imaging in live embryos—reduced reporter expression in the presence of *miR-153* and increased reporter expression upon knockdown of *miR-153* (Fig. 2C,D). In all cases, the effects were dependent on intact MREs. Taken together, the *in vivo* reporter assays and western blots support the conclusion that *snap-25* is a target of *miR-153*.

We next tested whether *miR-153* targets endogenous *snap-25*. Single cell embryos were injected with either *miR-153* or antisense morpholinos followed by western blots on pooled 1 dpf embryo lysates using antibodies against SNAP-25. Titration experiments were performed to optimize the levels of injected reagents (Figs. S4,S5). After optimization, protein levels were analyzed and fold changes in expression were determined compared to the amounts detected in noninjected controls (NIC) (Fig. 3). Under these conditions, excess *miR-153* led to a ~50% decrease in SNAP-25 levels whereas knockdown of endogenous *miR-153* increased SNAP-25 levels ~2-fold. To test for specificity we co-injected embryos with combinations of *miR-153*, *snap-25a,b* mRNAs, or morpholinos against both (Fig. 3). Injection of mRNAs encoding *snap-25a,b* resulted in a 2-fold elevation in SNAP-25 levels whereas injection of morpholinos that block the translation start site of *snap-25* led to a ~50% decrease in SNAP-25 levels. Importantly, co-injection of combinations of RNAs and morpholinos could suppress these effects and rescue SNAP-25 levels (Fig. 3). For both suppression experiments, the effects were dose dependent. Even though *snap-25a* was more effective than *snap-25b* at rescuing endogenous SNAP-25 levels, combinations both were the most effective (Fig. 3). These results indicate specific targeting of *snap-25* by *miR-153*. Although *miR-153* is likely to have additional targets, the ability to specifically rescue the effects of overexpression and knockdown of both *miR-153* and *snap-25* indicates that the effects we observe are specific to targeting of *snap-25* by *miR-153*.

miR-153 Regulates snap-25 to Control Movement

Because we could specifically suppress the effects of overexpression or knockdown of *miR-153* by co-injection of either *snap-25a,b* mRNA or morpholinos against *snap-25a,b*, we next sought to test whether the movement defects are caused by altered *miR-153* levels could likewise be rescued in a *snap-25* dependent manner. Embryonic movements were quantitated at 24 hpf after injection of antisense morpholinos against *snap-25* (*snap25*^{MO}) or with *snap-25a,b* mRNAs (Fig. 1; Movie S1). Knockdown of *snap-25* resulted in dramatically decreased embryonic movements, similar to overexpression of *miR-153* (Fig. 1). In contrast, overexpression of *snap-25a,b* increased movement approximately 5-fold over control NIC embryos (Fig. 1). For rescue experiments, co-injection of *snap-25a,b* mRNA with *miR-153* restored near normal movement (Fig. 1; Movie S1). Similarly, co-injection of morpholinos against both *snap-25* and *miR-153* also restored normal movement (Fig. 1; Movie S1). Thus, not only were SNAP-25 protein levels restored to normal, but also movement defects were rescued, demonstrating specific targeting of *snap-25* by *miR-153*.

SNAP-25 is a known target of Botulinum neurotoxin (BoNT) proteases A and E [8,9]. If *miR-153* is targeting *snap-25*, the effects of increased *miR-153* should mimic the effects of BoNT A. To test this prediction, injected zebrafish were exposed to BoNT A for 30 minutes at 27 hpf. One hour later, western blots were performed on pooled protein samples to determine whether it was possible to rescue SNAP-25 over-expression phenotypes associated with *miR-153* knockdown or injection of *snap25a,b* mRNAs. Exposure to BoNT A dramatically reduced SNAP-25 levels, recapitulating the effects of *miR-153* knockdown and over-expression (Fig. 4A,B). For movement, exposure to BoNT A rescued the hyperactive phenotypes observed after injection with MOs against *miR-153* or overexpression of *snap-25a&b* mRNAs (Fig. 4C; Movie S1). Together, these experiments strongly support the conclusion that *miR-153* specifically targets *snap-25* to regulate embryonic movement.

miR-153 Regulation of Motor Neuron Development

SNAP-25 is a well-characterized t-SNARE protein, with an established function in vesicular exocytosis [1–3]. In the developing nervous system, the SNARE complex mediates vesicular membrane addition driving neurite outgrowth and morphological patterning [1–3,35]. Moreover, DCV-mediated release of signaling proteins and growth factors is important for axon guidance, path finding, and morphological development [36–39]. We therefore sought to determine whether *snap-25* regulation by *miR-153* would alter neuronal morphogenesis. Because zebrafish motor neuron development is well characterized [40–45], we decided to focus on the effects of *miR-153* on motor neurons during early zebrafish development.

We first injected *miR-153* or morpholinos against *miR-153* to observe the effects on the development and morphology of motor neurons in a transgenic zebrafish line in which motor neurons are specifically labeled with RFP (*Tg(mx1:TagRFP-T)* [46]. Perturbation of *miR-153* levels caused striking changes in motor neuron structure and branching (Fig. 5A,B). Compared with NICs, overexpression of *miR-153* dramatically changed the axonal architecture with significant decreases in branch numbers and length (Fig. 5C, D). Knockdown of *miR-153* resulted in completely opposite effects with increased motor projection architectural complexity, increased axonal length, and increased branch numbers (Fig. 5B–D). To test whether the effects were specific, we conducted rescue experiments, as above. Injection of *snap-25a,b* mRNA or morpholinos against *snap-25a/b* produced virtually the same phenotypes observed in embryos subjected to *miR-153* knockdown or overexpression, respectively. In contrast, co-injection of *miR-153* and *snap-25a,b* mRNAs or morpholinos against *miR-153* and *snap-25a,b* almost completely restored the normal patterning and branching of motor neurons (Fig. 5B–D). These results indicate that *miR-153* regulates motor neuron development via control of *snap-25a,b*.

To further dissect the function of *miR-153* on motor neuron development, immunofluorescence was performed on whole-mount zebrafish embryos (55 hpf) with antibodies that label

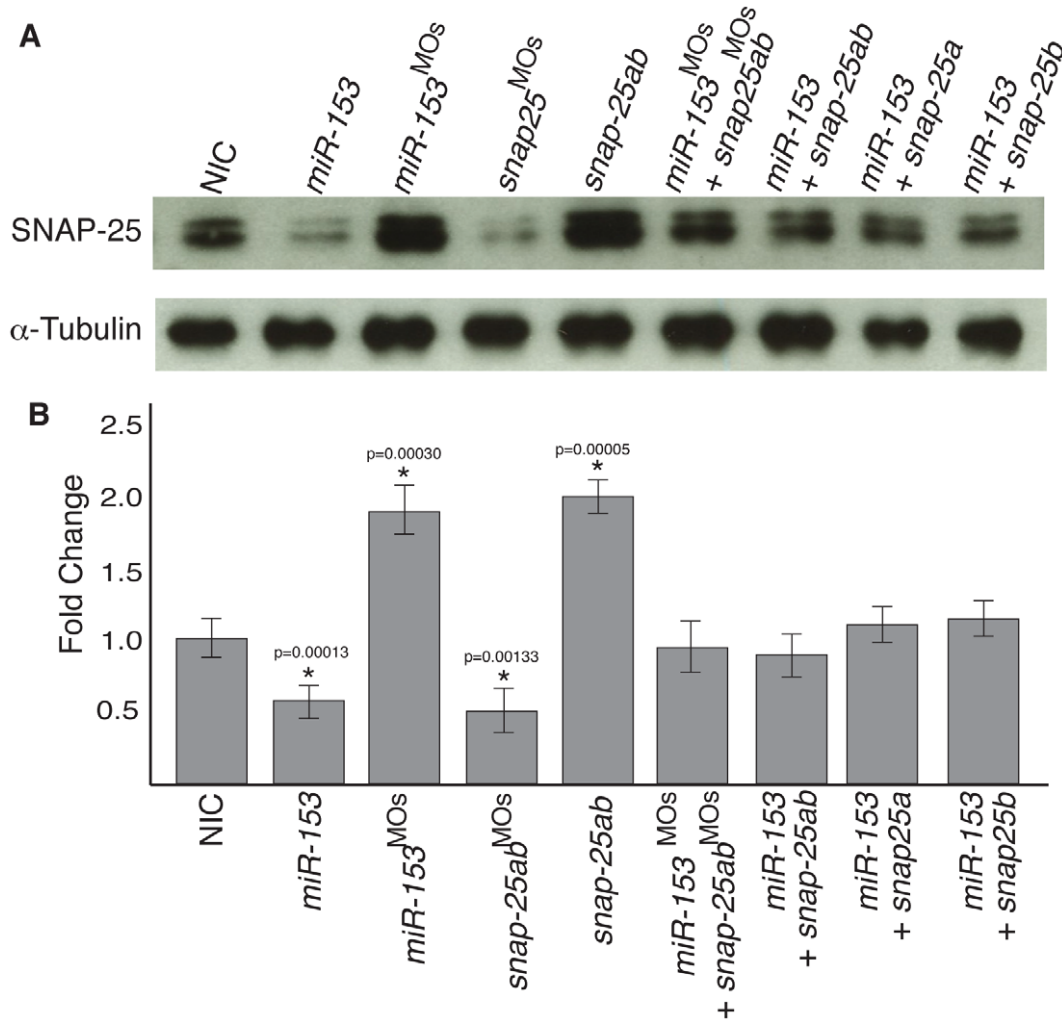


Figure 3. *miR-153* regulates endogenous *snap-25a* expression. (A) Embryo lysates were prepared from either NIC embryos or embryos injected with *miR-153*, *miR-153*^{MO}, mRNAs encoding *snap-25a* and *snap-25b*, morpholinos against *snap-25*, or combinations thereof, as indicated. Western blots were performed using antibodies against SNAP-25 and α -tubulin. (B) Quantification of SNAP-25 levels from the western blots (n = 3) shown in A. Significance was determined by a two-tailed Student's t-test. Error bars show s.e.m. doi:10.1371/journal.pone.0057080.g003

primary (Znp-1 or anti-synaptotagmin 2) or secondary (Zn-8 or Alcama) motor neurons [47]. Compared to NIC embryos, a striking difference in primary motor neuron axon architecture was observed with both *miR-153* overexpression (*miR-153*) and knockdown (*miR-153*^{MO}) (Fig. 6). A significant decrease in branching was observed in *miR-153* injected embryos whereas knockdown of *miR-153* caused a dramatic increase in branching. Likewise, injection of *snap-25a,b* mRNA led to increased axonal growth and branching in primary motor neurons whereas knockdown of *snap-25a,b* caused decreased outgrowth and branching (Fig. 6). Co-injection experiments showed that *snap-25a,b* mRNA and morpholinos against *snap-25* could partially counteract the effects of the corresponding gain and loss of *miR-153*.

For secondary motor neurons, rostral axon outgrowth was similarly stunted and/or irregularly spaced by *miR-153* overexpression and slightly elongated by *miR-153* knockdown (Fig. S6). Differences in the caudal region were minimal compared to earlier developing rostral neurons, possibly reflecting temporal limitations to injection experiments or perhaps increased vulnerability of rostral motor neurons to altered SNAP-25 levels. Focusing on

rostral effects, injection of *snap-25a,b* mRNA phenocopied *miR-153* knockdown and injection of morpholinos against *snap-25* resulted in patterns that closely resembled *miR-153* overexpression. Co-injection of morpholinos against both *miR-153* and SNAP-25 largely restored normal secondary motor neuron patterning, although the injection of *snap-25a,b* mRNAs was not as effective at rescuing the defects that resulted from *miR-153* overexpression (Fig. S6). This may indicate a possible additional function for *miR-153* in regulating axonal growth and patterning during secondary motor neuron development.

Expression of *miR-153* in Motor Neurons

To ensure that the effects of *miR-153* on motor neuron patterning were due to expression of *miR-153* in these cells, we FACS sorted cells from the trunks of 52 hpf (*Tg(mmx1:TagRFP-T)*) embryos and conducted RT/qPCR. As shown in Fig. 7, there was a greater than 10-fold enrichment for *miR-153* in RFP+ cells compared to RFP- cells. Prior work had shown that *miR-153* is expressed in the brain and spinal cord but these results show that *miR-153* is expressed in developing motor neurons.

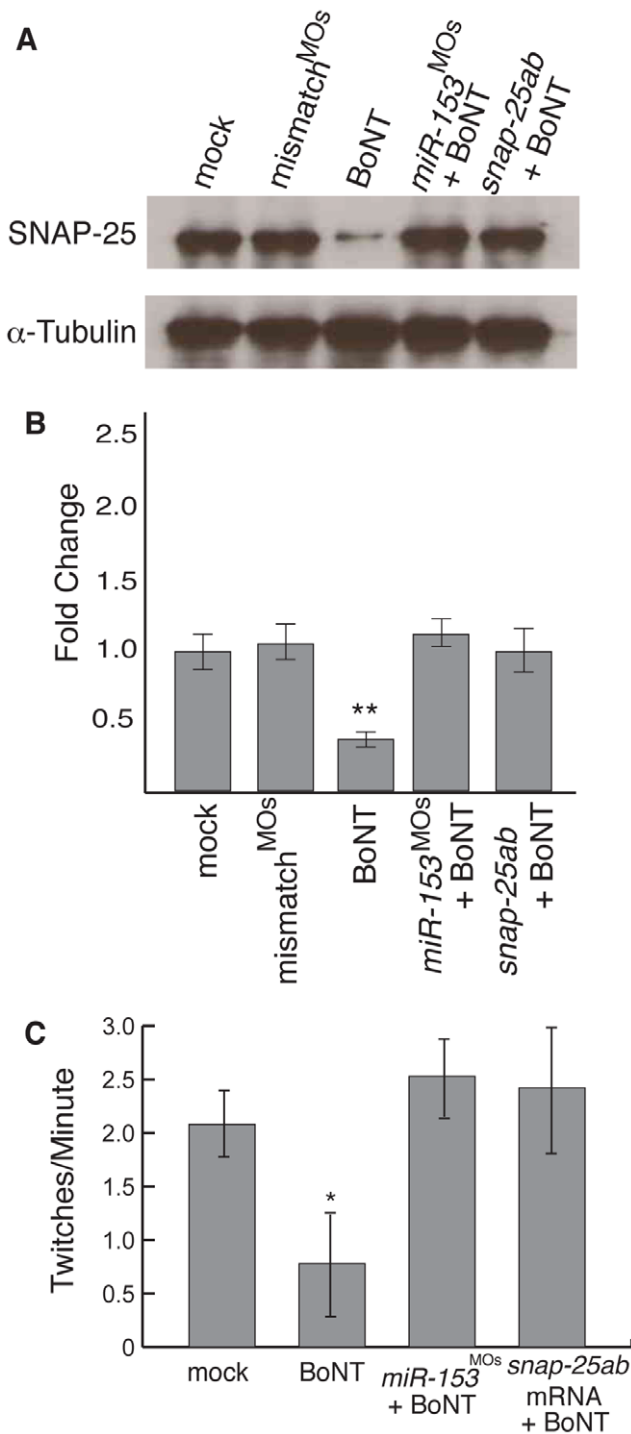


Figure 4. *miR-153* mimics the effects of BoNT A. (A) Single cell embryos were injected as indicated and then at 27 hpf, exposed to Botulinum neurotoxin A (BoNT) for 30 minutes. After recovery for 1 hour, western blots were performed on embryo lysates using antibodies against SNAP-25 or α -tubulin. (B) Quantitation of SNAP-25 levels from A, $n=3$. **, $p<0.01$. (C) Embryonic movement in the presence or absence of BoNT A. The number of twitches per minute was counted as in Fig. 1 for embryos treated as indicated. Significance was determined by comparing mock embryos to all other conditions using ANOVA with Dunnett's post-test, $n=15$. *, $p<0.05$. doi:10.1371/journal.pone.0057080.g004

miR-153 Regulates Vesicular Exocytosis to Control Signaling

Since SNAP-25 has a well-established function in the fusion and release of numerous vesicle types, we next examined the role that *miR-153* plays in modulating exocytosis. Owing to the core role of *miR-153* in movement control, we first focused on synaptic activity at the neuromuscular junction (NMJ) in zebrafish embryos. For this analysis, we measured synaptic vesicle (SV) cycling using the styryl dye, FM1-43 [48,49]. At 55 hpf, embryonic NMJs were imaged with Alexa 594-conjugated α -bungarotoxin (α -Btx) to label postsynaptic acetylcholine receptor (AChR) clusters, while monitoring FM1-43 uptake into NMJ presynaptic boutons (Fig. 8). The terminals were acutely depolarized for 5 minutes with high $[K^+]$ saline (45 mM) to drive the SV cycle and load FM1-43, whereas only weak loading was evident in low $[K^+]$ conditions. In non-injected controls, fluorescence was observed along terminal axon branches with intense staining at individual synaptic varicosity boutons (Fig. 8A). Compared to NIC labeling, *miR-153* overexpression resulted in a significant decrease in FM1-43 loading in presynaptic terminals, indicating slowing of the SV cycle (Fig. 8B). In sharp contrast, knockdown of *miR-153* showed a significant increase in FM1-43 loading, indicating an elevated SV cycling rate (Fig. 8C). The significant difference between *miR-153* knockdown and overexpression conditions indicates that *miR-153* plays an important role in controlling the rate of vesicle cycling (Fig. 8D). Together, these results reveal a key function for *miR-153* in the control of presynaptic vesicle release at the embryonic NMJ, consistent with a role for *miR-153* in the regulation of embryonic movement. The overall effects on movement are therefore a combination of effects on motor neuron development and patterning as well as overall exocytic activity.

SNAP-25 has a highly conserved role mediating vesicular fusion in both neurons and other neurosecretory cells where it is critical for DCV release [50]. To test whether *miR-153* plays a role in this secretory context, we examined exocytosis in a rat neuroendocrine pituitary cell line (GH4C1) expressing human growth hormone (hGH) [51]. Release of hGH in these cells provided a functional readout of exocytic activity (Fig. 9). GH4C1 cells were therefore transfected with *miR-153*, morpholinos against *miR-153/snap-25*, or vectors expressing *snap-25a,b*, followed by determination of hGH levels in the media by ELISA. Overexpression of *miR-153* and knockdown of *snap-25a,b* (*snap-25a,b*^{MO}) reduced the levels of hGH to below the amount detected in culture media from mock transfected cells (Fig. 9). In sharp contrast, knockdown of *miR-153* and overexpression of *snap-25* both significantly increased the amount of secreted hGH 8–10 fold over the mock transfected control (Fig. 9). The differences observed due to perturbation of *miR-153* levels in the GH4C1 cell line compared to embryonic NMJs are most likely due to differences in the efficiency of *miR-153/miR-153*^{MO} delivery between the two experiments, as well as developmental differences. Nevertheless, the effects in this case were fully suppressed by co-expression of either *miR-153/snap-25a,b* mRNA or MOs against *miR-153/snap-25a,b*, demonstrating specific regulation of *snap-25* by *miR-153*. These data strongly support the conclusion that *miR-153* functions to precisely control SNAP-25 levels to regulate vesicle exocytosis.

Discussion

In this study, we show that *miR-153* regulates the critical core SNARE component, SNAP-25, to modulate exocytosis and neuronal development. Increased *miR-153* levels cause decreased SNAP-25 expression resulting in decreased embryonic movement, decreased neuronal secretion, and decreased neuronal growth/

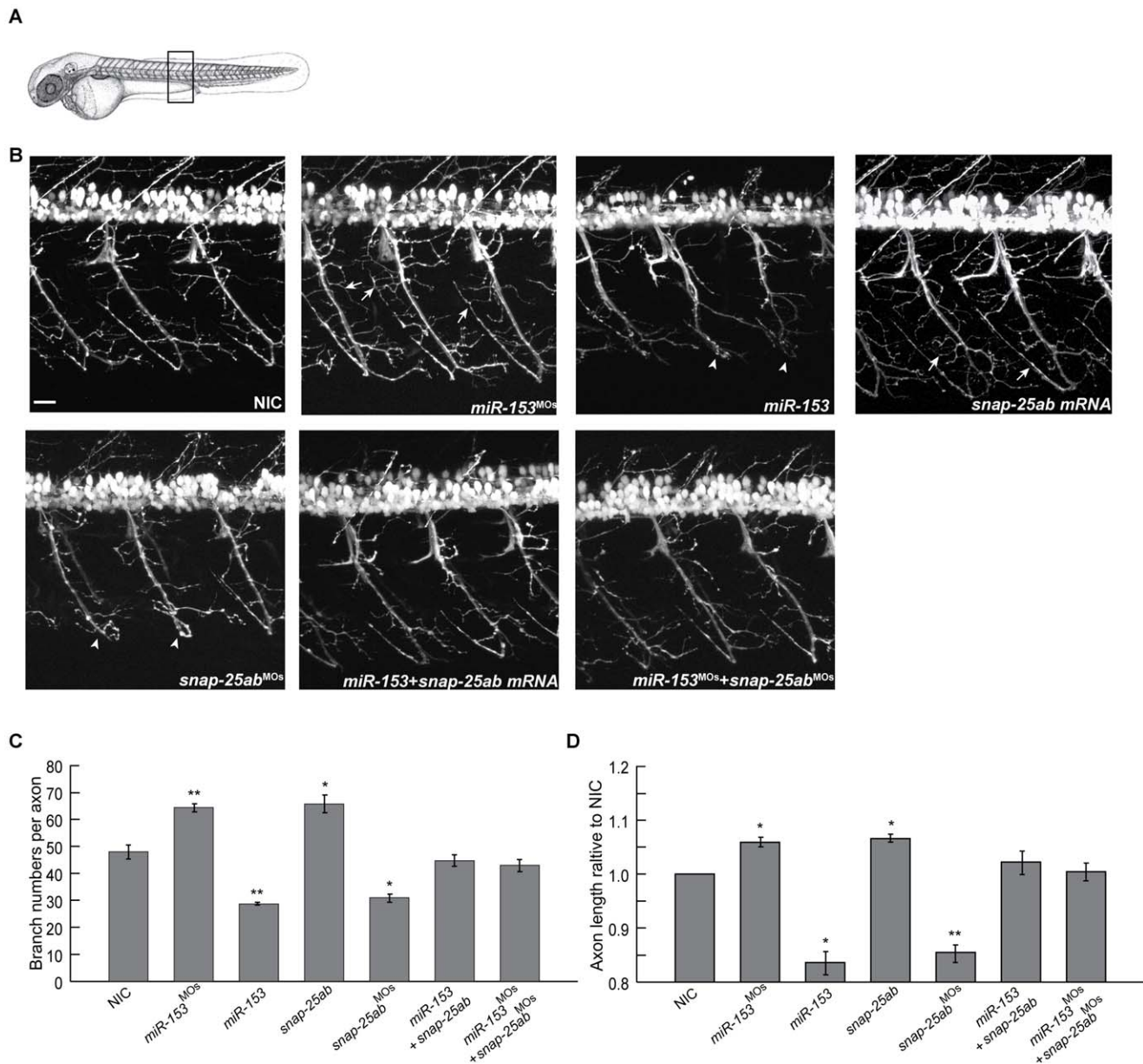


Figure 5. *miR-153* regulates the morphology and structure of motor neurons. (A) A transgenic zebrafish line, *Tg(mnx1:TagRFP-T)*, that expresses RFP in motor neurons was used to monitor the effects of altered levels of *miR-153* and *snap-25* at 55 hpf. For all confocal images, developing motor neurons were examined from the same somites, as indicated. (B) Morphology of developing motor neurons under each of the indicated conditions. Arrows indicate increased branching after knockdown *miR-153* (*miR-153^{MOs}*) or overexpression *snap-25a,b* mRNA. Arrowheads indicate the structural defects after *miR-153* overexpression or knockdown of *snap-25a,b* (*snap-25a,b^{MOs}*). Scale bar: 20 μ m. (C) Quantification of motor neuron axonal branch number under the different conditions shown in (B). Error bars show s.e.m. Significance was determined using ANOVA with Dunnett's post-test, $n=5$. *, $p<0.01$; **, $p<0.005$. (D) Quantification of motor neuron axon length relative to uninjected control under the different conditions shown in (B). Error bars show s.e.m. ANOVA with Dunnett's post-test, $n=5$. *, $p<0.05$; **, $p<0.01$. doi:10.1371/journal.pone.0057080.g005

branching. Conversely, *miR-153* knockdown causes elevated SNAP-25 expression resulting in hyperactive movement, increased neuronal secretion, and increased neuronal growth/branching. Accumulating evidence suggests that SNAP-25 misregulation plays a role in numerous human disease states including ADHD, schizophrenia, bipolar I disorder, Huntington's disease, Alzheimer's disease, and diabetes [52]. Regulated expression of *miR-153* provides an attractive model to mechanistically explain tight control of SNAP-25 levels.

SNAP-25 Functions during Development

It is well established that axon outgrowth during neuronal development occurs via SNARE-dependent addition of membrane for growth cone extension [35,53]. Axonal growth, pathfinding, and target recognition are secondarily modulated by SNARE-dependent release of developmental signals via dense core vesicle (DCV) exocytosis [54–59]. The outgrowth of both axons and dendrites is blocked by Botulinum neurotoxins A and C1, proteases specific for SNAP-25, demonstrating a direct role of SNAP-25 in neuronal morphogenesis [55,56,60]. Likewise, in-

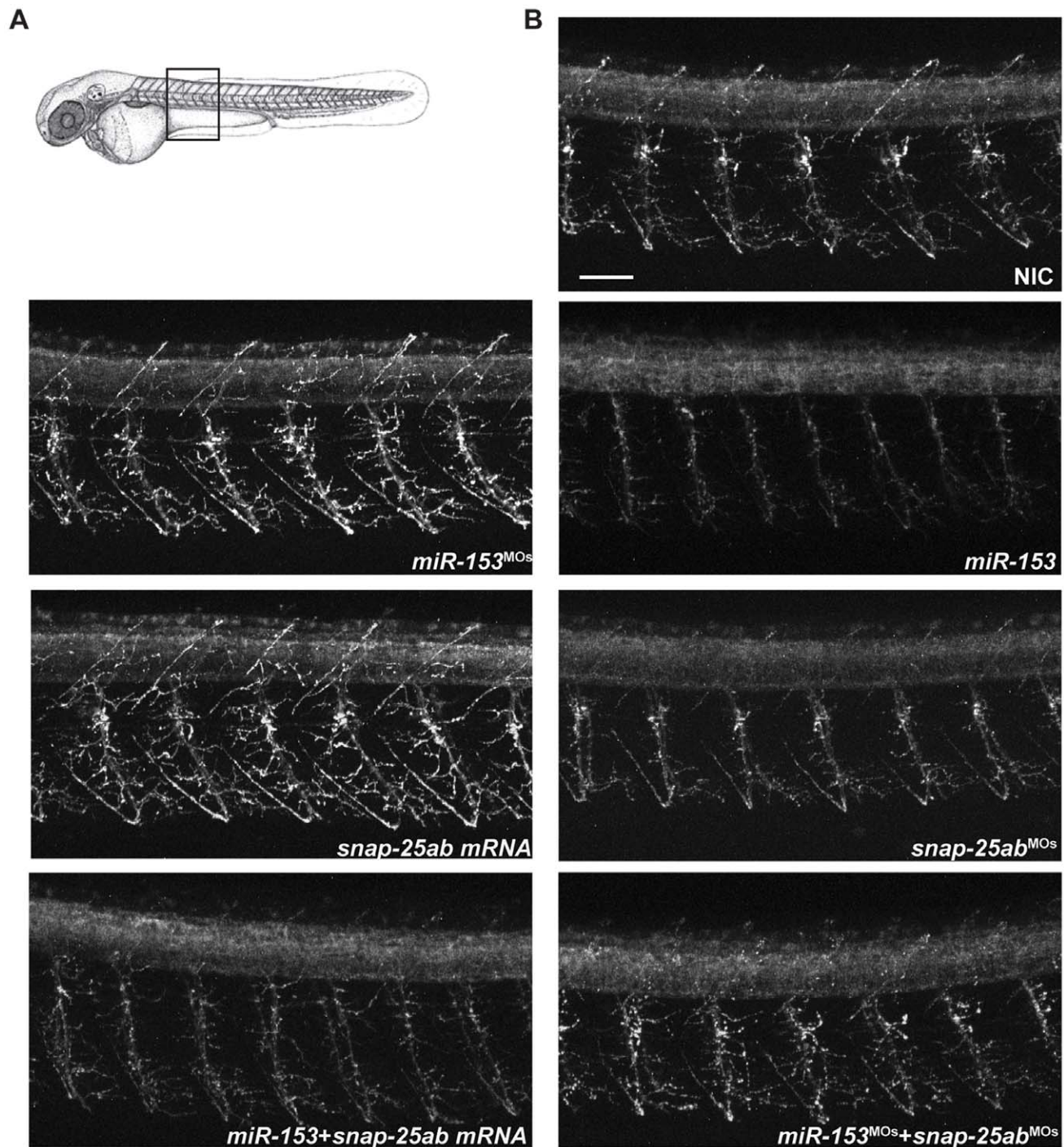


Figure 6. *miR-153* regulates primary motor neuron development. (A) Immunofluorescence performed on whole mount zebrafish embryos at 55 hpf using Znp-1 antibodies to label primary motor neurons. Confocal images were acquired from the same somites for all embryos, as indicated. (B) Effects on primary motor neuron structure and branching under the indicated conditions. Scale bar: 40 μ m. doi:10.1371/journal.pone.0057080.g006

hibition of SNAP-25 by antisense oligonucleotides blocks axonal outgrowth [54]. In stark contrast, neuronal outgrowth was surprisingly not inhibited in SNAP-25 null mice [13]. The explanation for this inconsistency is not clear. Our results show a clear requirement for SNAP-25 in motor neuron outgrowth and branching in zebrafish. It is possible that the requirement for SNAP-25 may be species specific but we found that altered levels of *miR-153* caused similar branching defects in rat PC12 cells as

observed in zebrafish motor neurons, strongly arguing against this (data not shown). Perhaps the differences are due to cell-specific requirements for SNAP-25. In the retina, for example, SNAP-25 is expressed in a dynamic spatiotemporal pattern and such differential expression may underlie specific development of cholinergic amacrine cells and photoreceptors [61]. An intriguing possibility based on the results presented here is that developmental, stage-specific and/or cell-specific expression of *miR-153*

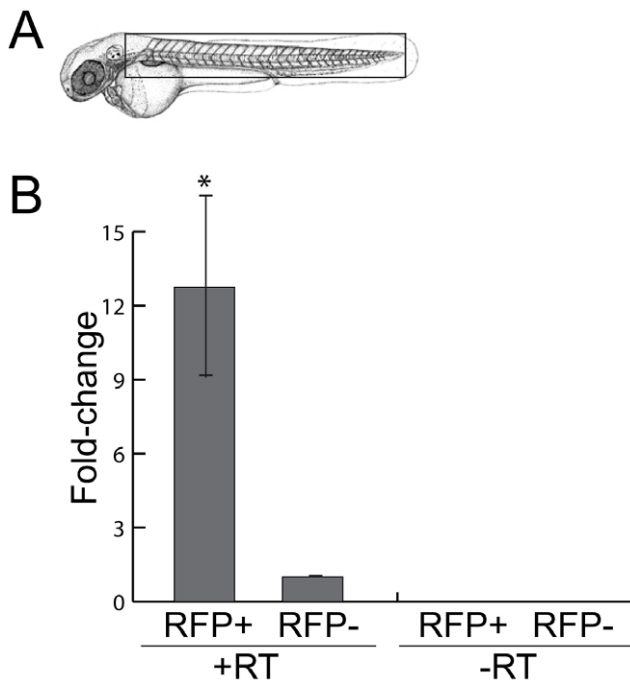


Figure 7. *miR-153* is expressed in motor neurons. To enrich for motor neurons, heads were removed from 52 hpf embryos just posterior to the otic vesicle and trunks were dissociated to facilitate sorting of RFP+ and RFP- cells. RNA was isolated from these cell fractions and RT/PCR was performed to determine *miR-153* levels relative to U6 snRNA. Significance was determined by a two-tailed Student's t-test with the error bars representing s.e.m.; $p < 0.02$. doi:10.1371/journal.pone.0057080.g007

may similarly regulate SNAP-25 levels, which then drives developmental and cell-specific effects.

SNAP-25 in Synaptic Vesicle Exocytosis

SNAP-25 is one of three SNARE proteins that contribute α -helices that mediate fusion between synaptic vesicles and pre-synaptic membranes [1,3]. Blockage of synaptic transmission by Clostridium and Botulinum neurotoxins first established that SNARE proteins are critical for neurotransmitter release [62]. Cleavage of SNAP-25 by Botulinum neurotoxin A causes a paralytic phenotype that resembles the loss of movement we observe in zebrafish embryos expressing excess *miR-153*. SNAP-25 haploinsufficient mice show no observable phenotypic defects but complete loss of SNAP-25 blocks evoked synaptic transmission [13]. Moreover, overexpression of SNAP-25 inhibits normal calcium responsiveness and can impair memory-associated synaptic plasticity [63]. These findings suggest that modulation of SNAP-25 levels are important for overall SNARE function, especially in generating differences in calcium dependence between neuronal and non-neuronal secretory vesicular fusion events. Matteoli and colleagues (2009) have shown that SNAP-25 is differentially expressed between excitatory glutamatergic and inhibitory GABAergic neurons in a developmental-specific manner [4]. These results remain controversial, as earlier studies did not observe this difference, but the data are consistent with an important role for SNAP-25 as a required component for both glutamatergic and GABAergic transmission [64,65]. Mechanisms for how SNAP-25 levels might be regulated in a development-and/or cell-specific manner are uncertain, but our data strongly support miRNA regulation as a likely candidate and a critical

mechanism controlling SNAP-25 levels. A recent report describing the effects of chronic overexpression of SNAP-25 in the rat dorsal hippocampus demonstrated the critical importance of controlling SNAP-25 levels [63]. Elevated expression of SNAP-25 produced increased levels of secreted glutamate with cognitive deficits similar to those observed in ADHD and schizophrenia. We propose that *miR-153* control of SNAP-25 levels allows for precise regulation of SNAP-25 during development and exocytosis.

miRNAs Regulation of Neuronal Morphogenesis and Synaptic Activity

Localized translation control in synaptic dendrites is common, requiring repression of mRNA translation during transport. miRNA mediated inhibition of translation is an attractive mechanism that can precisely control gene expression in neurons. Consistent with this hypothesis, many miRNAs are neuron or brain specific [66]. Moreover, the effector complexes that carry out repression of translation (RNA Induced Silencing Complexes; RISCs) are composed of several subunits that have been implicated in both neuronal function and disease [22,24,67]. For example, nervous system specific miRNAs have been shown to regulate the maturation of dopamine neurons in the midbrain as well as control serotonin transport by regulating the serotonin transporter [68,69]. Likewise, *miR-1*, *miR-124*, *miR-125b*, *miR-132*, *bantam*, *miR-34* and the *miR-310* cluster have all been implicated in the modulation of synaptic homeostasis [70–76]. Similarly, synaptic plasticity is reportedly regulated by *miR-134* through targeting of SIRT1 or Limk1, which control dendritic spine morphogenesis [77,78]. In addition, *miR-124* in retinal ganglion cell growth cone was shown to act through CoREST to regulate the intrinsic temporal sensitivity to Sema3A, a guide cue during axonal pathfinding and morphogenesis [79]. Our work demonstrates that *miR-153* is a member of this subset of miRNAs implicated in neuronal function but by a distinctly different mechanism through targeting of *snap-25*. *miR-153* also likely targets other mRNAs [80], but SNAP-25 regulation alone is required and sufficient to explain the role of *miR-153* regulation of movement, motor neuron morphogenesis, and SNARE-mediated secretion.

Materials and Methods

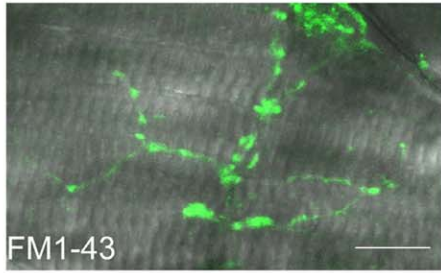
Ethics Statement

The Animal Care and Use Committee monitors all animal care and research at Vanderbilt. Vanderbilt University has on file with the Office for Protection from Research Risks of the NIH an Assurance of Compliance with Public Health Service regulations and requirements and provisions of the Animal Welfare Act. All zebrafish experiments in this paper were approved by the Vanderbilt University Institutional Animal Care and Use Committee (IACUC) under protocol M-09-398. In accordance with that protocol, all necessary means were taken to avoid pain. For any manipulations that might induce pain, animals were anesthetized with a 0.15% solution of Tricaine (3-amino-benzoic acid ethylester). The approved method for euthanizing zebrafish is incubation in ice water.

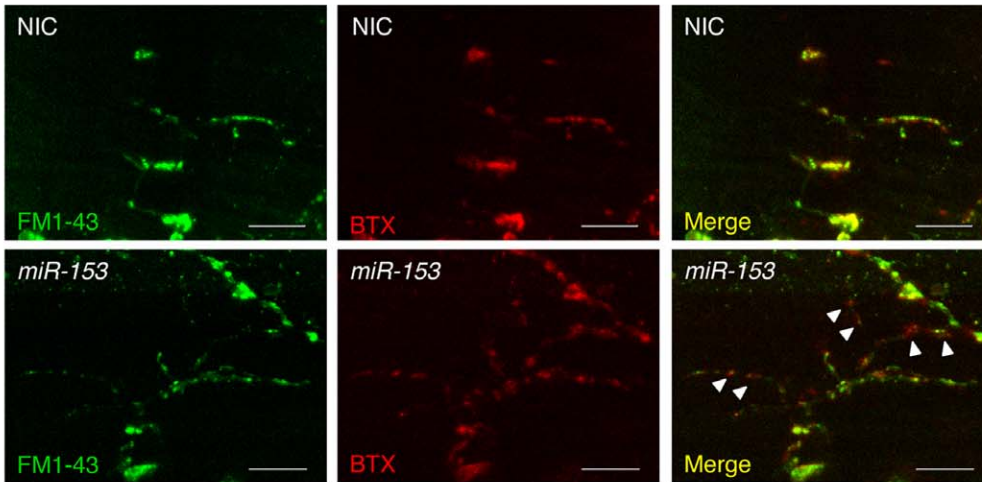
Microinjections

Single cell zebrafish male and female embryos were injected with 200 pg of *miR-153*, 5 ng each of *miR-153^{MO}* and *miR-153^{loop^{MO}}* and/or 100 pg of *in vitro*-transcribed, capped GFP reporter mRNA with or without the *snap-25a* or *b* 3'UTR. Zebrafish *snap-25a,b* 3' UTR sequences were amplified by PCR and subcloned downstream of the GFP ORF in pCS2+ [81].

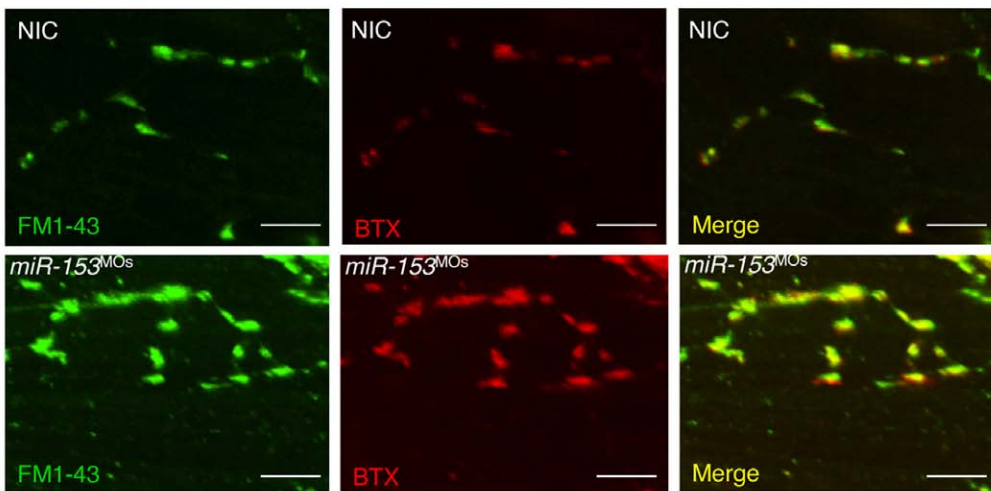
A



B



C



D

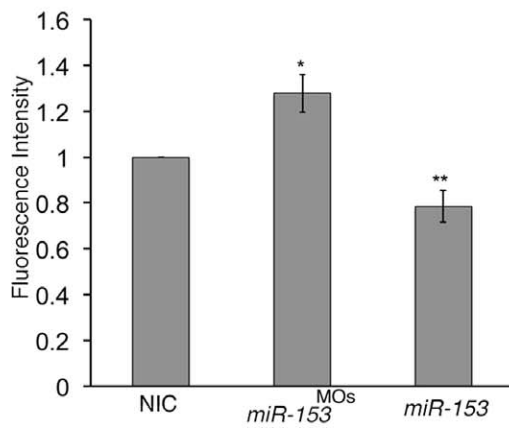


Figure 8. miR-153 regulates synaptic activity at the neuromuscular junction. (A) FM1-43 loading of neuromuscular junction (NMJ) boutons in 55 hpf fish embryos. (B) Postsynaptic clusters of AChRs were labeled with Alexa 594-conjugated α -bungarotoxin. Overexpression of *miR-153* caused decreased FM1-43 loading, indicating down-regulation of the synaptic vesicle cycle within NMJ boutons (arrowheads). (C) Knockdown of *miR-153* (*miR-153*^{MO}) promoted greater uptake of FM1-43 dye, indicating increased synaptic vesicle cycling. Scale bar: 10 μ m. (D) Quantification of FM1-43 fluorescent intensity with a paired Student's t-test. Error bars show s.e.m. * $p < 0.01$; ** $p < 0.02$. doi:10.1371/journal.pone.0057080.g008

Rescue experiments used injections of 3 ng of *snap-25*^{StartMO} and *snap-25*^{5'UTRMO}, 150 pg of *snap-25a,b* mRNA, 250 pg of *snap-25a* mRNA, or 300 pg of *snap-25b* mRNA without 3'UTRs.

Two different morpholinos against *miR-153* were utilized. One was perfectly complementary to the mature sequence; the second was complementary to a portion of the mature sequence and then extending into the precursor loop. Targeting of *snap-25a,b* mRNAs was performed using morpholinos against the region including the start codon.

Botulinum Toxin Analysis

Embryos injected at the 1-cell stage were treated with purified Botulinum neurotoxin A (Metabio, Inc., Madison, WI). Initial titration experiments were performed testing a range of BoNT A concentrations with final selection of 1 ng per 10 ml of water for 30 minutes at either 24-hpf or 48-hpf. Embryos were washed 10 times in fresh water and then allowed to recover for 1 hour prior to protein extraction or video capture to monitor movement.

qRT-PCR and Northern Blots

Total RNA extracted from both RFP+ and RFP- cells was reverse transcribed and qPCR reactions were carried out using Taqman miRNA assays (Life Technologies, NY) using the CFX96 Real-time PCR system (Bio-Rad), as previously described [32]. Northern blots were also performed as described [82,83].

Western Blots

Embryos were dechorionated, deyolked, and sonicated in lysis buffer as described [83]. Approximately 100 embryos were pooled and one-tenth of the resulting samples were loaded into each lane. Membranes were probed with antibodies against α -tubulin (Abcam, ab15246), GFP (Torrey Pines, TP401) or SNAP-25 (Alomone Labs). For detection, anti-rabbit or anti-mouse HRP-conjugated secondary antibodies were used, followed by visualization with ECL.

GFP Reporter Analyses

Reporter analyses and western blots were as described [83]. To generate the *snap-25a,b* GFP reporters, the GFP ORF was fused to the 3' UTR sequence of zebrafish *snap-25a* or *b*. *snap-25a,b* UTRs were cloned from zebrafish whole embryo RNA preparations using oligo d(T) primed reverse transcription followed by PCR amplification with gene specific primers. Images were acquired with a Leica MZFIH dissecting scope equipped with a fluorescent laser using a Qimaging camera with Qimaging software and imported into Adobe Photoshop for orientation and cropping.

Immunofluorescence

Embryos were fixed in 4% PFA overnight at 4°C and then permeabilized in 0.5% TritonX-100 for 60 minutes followed by treatment with protease K (20 μ g/ml) for 10 minutes at room temperature. Samples were washed in PBT-DMSO before blocking overnight at 4°C (PBT-DMSO, 2% BSA, 5% goat serum). Primary antibodies (SNAP-25, 1:1000; SV-2, 1:300; ZNP-

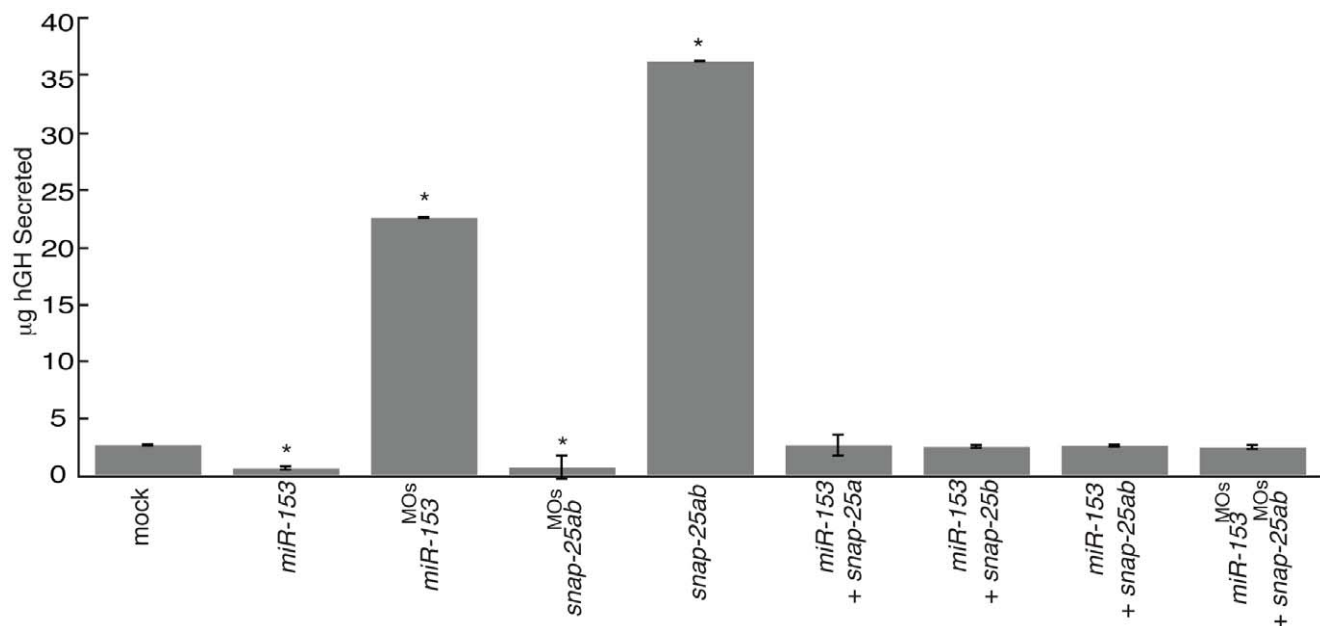


Figure 9. miR-153/snap-25 regulates vesicular exocytosis. GH4C1 cells stably expressing human growth hormone (hGH) were transfected, as indicated. The effects of exogenous expression on hGH levels secreted into the culture media were determined by ELISA using hGH antibodies. Significance was determined by comparing mock transfected to all other treatments using ANOVA with Dunnett's post-test. Error bars show s.e.m. *, $p < 0.01$.

doi:10.1371/journal.pone.0057080.g009

1, 1:2000; ZN-8, 1:25) were incubated overnight at 4°C, washed with PBT-DMSO, and then embryos were incubated with Cy5 or Cy3-conjugated donkey anti-mouse or rabbit antibodies (Jackson Immuno) for 4 hrs at room temperature. Before mounting and visualization, embryos were washed with PBT-DMSO. PC12 cells were fixed in 4% PFA for 15 mins, washed in PBS before incubating with primary antibodies for 1 hr, washed, incubated with secondary antibodies for 1 hr, Hoechst dye for 5 mins, washed, and visualized.

Tissue Dissociation and Motor Neuron Isolation

Tg(mnx1:TagRFP-T) zebrafish embryos of 52 hpf were dechorionated, deyolked, and then dissected just posterior to the otic vesicle to collect trunks (excluding the hearts). Tissues were kept in buffer (1×PBS, pH 6.4, 1%BSA) and then dissociated using 16 U/ml papain and 0.2 U/ml Dispase (Worthington, NJ) for 30 mins at 28°C on a rotator. After complete dissociation of the tissue by careful pipetting up and down, cells were pelleted at 8000×g for 2 mins. Resuspended cells were then treated with 1 mg/ml leupeptin (Worthington, NJ) and 100 U/ml DNaseI (Sigma-Aldrich) in PBS at pH 7.4 containing 2 mg/ml MgCl₂ for 10 mins at room temperature and then kept on ice for RFP+ and RFP- cell isolation. Gating was based on cell size and fluorescence intensity, determined by the control sample of dissociated cells from WT fish at the same developmental stage.

FM1-43 Dye Labeling

Embryos at 55 dpf were incubated in HBSS (137 mM NaCl, 5.4 mM KCl, 1 mM MgSO₄, 0.44 mM KH₂PO₄, 0.25 mM Na₂HPO₄, 4.2 mM NaHCO₃, 1.3 mM CaCl₂, 5 mM Na-HEPES) containing 0.2% Tricaine and glued onto sylgard coated glass chambers before removing the skin using a glass needle. FM1-43 and α -bungarotoxin (α -Btx) labeling procedures were as previously published [49], except the preloading incubation of FM1-43 dye was omitted and the Advasep incubation period was elongated to 15 mins. For data analysis, axons with puncta labeled with α -Btx were considered as synaptic boutons. FM1-43 puncta with sizes of 0.5–2 μ m were collected for analysis using Image J.

Cell Culture and ELISA

PC12 cells (ATCC CRL-1721) were maintained using Ham's F12K media with 15% horse serum and 5% FBS, and transfected individually or in combination with miRNAs, mRNAs, and morpholinos. Transfections were performed with 300 nM *miR-153*, biotinylated *snap-25* MOs and *miR-153* MOs and 1.5 μ g of *snap-25a,b* using Lipofectamine 2000 [84]. Co-transfection of a GFP plasmid was used to determine transfection efficiencies. Efficiencies less than 50% were discarded. One day after transfection, 50 ng/ml nerve growth factor was added to media to induce differentiation. Neurite outgrowth was assayed at day 5 by immunostaining with antibodies against acetylated α -tubulin. Stably transfected GH4C1 cells were a gift from Dr. K. Kannenberg [51]. ELISAs were performed after 5 days of transfection and human growth hormone was assayed following the Diagnostic Systems ELISA kit.

Supporting Information

Figure S1 Northern blot of *miR-153* overexpression and knockdown. Perturbation of *miR-153* expression levels by injection of *miR-153* or MOs against different regions of pre-*miR-153* was verified by northern blot. U6 served as a loading control. (TIF)

Figure S2 Conservation of *snap-25* 3' UTR sequences. The 3' UTRs from mouse, human and zebrafish *snap-25a* (A) and *snap-25b* (B) are shown with the MREs that pair with *miR-153* boxed in green. Conserved nucleotides are marked by an asterisk. The exact pairings between the MREs and *miR-153* are shown in Figure 2 and Figure S3. Despite different levels of conservation, both MREs in *snap-25a* pair extensively with *miR-153* in the seed region. (TIF)

Figure S3 *miR-153* targets *snap-25b*. (A) GFP reporter constructs were created by fusing the reading frame of GFP to the *snap-25b* 3'UTR. Three predicted miRNA recognition elements (MREs) were identified in the *snap-25b* 3' UTR. The *miR-153* sequence is indicated in red and the corresponding *snap-25a* UTR sequence is shown in green. (B) Single cell zebrafish embryos were injected with mRNAs derived from GFP reporters lacking a UTR (GFP), fused to the full length *snap-25b* UTR (GFP+*snap-25b*), or mutant version of the *snap-25b* UTR lacking all MREs (GFP+*snap-25b* Δ MRE1, 2&3). Embryos were injected in the presence or absence of exogenous *miR-153* or morpholinos against *miR-153* (*miR-153*^{MO}). Fluorescence levels were examined at 1 dpf. Clusters of embryos (~30) are shown. (C) Lysates from ~100 embryos were prepared from embryos treated as in B and GFP protein levels were determined by western blotting using antibodies against GFP or control antibodies against α -tubulin. (TIF)

Figure S4 Dose-dependent rescue of *miR-153* knock-down. (A) Single cell embryos were injected with a constant level of *miR-153*^{MO} and increasing amounts (increments of 2 ng) of *snap-25*^{MOs}. Embryo lysates from ~60 embryos in each group were prepared and SNAP-25 protein levels determined by western blotting. (B) Quantitation of westerns (n = 3) from A. The grey circle represents the amount of *snap-25*^{MO} (10 ng) used in co-injection rescue experiments. (TIF)

Figure S5 Dose-dependent rescue of *miR-153* over-expression. (A) Single cell embryos were injected with a constant level of *miR-153* and increasing amounts (increments of 50 pg) of *snap-25a*, *snap-25b*, or *snap-25a&b* mRNA. Embryo lysates from ~60 embryos were prepared from embryos in each treatment group and SNAP-25 protein levels were determined by western blotting. (B) Quantitation of westerns (n = 3) from A. The grey circles represent the amounts used in co-injection rescue experiments (75 pg each of *snap-25a* and b, 250 pg of *snap-25a*, and 300 pg of *snap-25b*). (TIF)

Figure S6 *miR-153* regulates secondary motor neuron development. (A) Immunofluorescence was performed on whole mount zebrafish embryos at 55 hpf using Zn-8 antibodies to label secondary motor neurons. Confocal images were acquired from the same somites for all embryos, as indicated. (B) *miR-153* knockdown (*miR-153*^{MO}) and *snap-25a,b* overexpression significantly increased the growth of secondary motor neuron axons (arrows). Overexpression of *miR-153* or knockdown of *snap-25a,b* (*snap-25a,b*^{MO}) caused severe defects in axon development and architecture (asterisks). Scale bar: 40 μ m. (TIF)

Movie S1 Embryo Movements in different conditions. 0:00–0:11. NIC Embryo Movements at 24 hpf Noninjected control (NIC) zebrafish embryos at 24 hpf were filmed for one minute. Twitching was counted from individual embryos over multiple movies, as quantitated in Figure 1. **0:11–0:21. Effects**

of miR-153 Overexpression on Movement at 24 hpf Single cell zebrafish embryos were injected with *miR-153* and filmed for one minute at 24 hpf. Twitching was counted from individual embryos over multiple movies, as quantitated in Figure 1. **0:22–0:32. Effects of Knockdown of miR-153 on Movement at 24 hpf** Single cell zebrafish embryos were injected with *miR-153^{MOs}* and filmed for one minute at 24 hpf. Twitching was counted from individual embryos over multiple movies, as quantitated in Figure 1. **0:33–0:42. Effects of Decreased SNAP-25 Expression on Movement at 24 hpf** Single cell zebrafish embryos were injected with *snap-25a,b^{MO}* and filmed for one minute at 24 hpf. Twitching was counted from individual embryos over multiple movies, as quantitated in Figure 1. **0:42–0:52. Effects of Increased SNAP-25 Expression on Movement at 24 hpf** Single cell zebrafish embryos were injected with *snap-25a,b* mRNA and filmed for one minute at 24 hpf. Twitching was counted from individual embryos over multiple movies, as quantitated in Figure 1. **0:52–1:02. Effects of co-Injection of miR-153 and snap-25a,b on Movement at 24 hpf** Single cell zebrafish embryos were co-injected with *miR-153* and *snap-25a,b* mRNA and filmed for one minute at 24 hpf. Twitching was counted from individual embryos over multiple movies, as quantitated in Figure 1. **1:02–1:12. Effects of co-Injection of miR-153^{MO} and snap-25a,b^{MO} on Movement at 24 hpf** Single cell zebrafish embryos were co-injected with *miR-153^{MO}* and *snap-25a,b^{MO}* and filmed for one minute at 24 hpf. Twitching was counted from individual embryos over multiple movies, as quantitated in Figure 1. **1:12–1:22. NIC Embryo Movements at 28 hpf** Noninjected control (NIC) zebrafish embryos at 28 hpf were filmed for one minute at the same time that the following Movies were created. Twitching was counted from individual embryos, as quantitated in Figure 4C. **1:22–1:32. Effects of Botulinum Toxin Treatment on**

Movement at 28 hpf Single cell zebrafish embryos were injected with injection dye and treated with Botulinum toxin A at 27 hpf. After a 30 min treatment, embryos were washed and allowed to recuperate for 1 hour before being filmed. Twitching was counted from individual embryos, as quantitated in Figure 4C. **1:33–1:42. Effects of Botulinum Exposure and co-Injection of miR-153^{MO} on Movement at 28 hpf** Single cell zebrafish embryos were injected with *miR-153^{MOs}* and treated with Botulinum toxin A at 27 hpf. After a 30 min treatment, embryos were washed and allowed to recuperate for 1 hour before being filmed. Twitching was counted from individual embryos, as quantitated in Figure 4C. **1:42–1:52. Effects of Botulinum Exposure and co-Injection of snap-25a,b mRNA on Movement at 28 hpf** Single cell zebrafish embryos were injected with *snap-25a,b* mRNA and treated with Botulinum toxin A at 27 hpf. After a 30 min treatment, embryos were washed and allowed to recuperate for 1 hour before being filmed. Twitching was counted from individual embryos, as quantitated in Figure 4C. (MOV)

Acknowledgments

We thank Drs. Sarah Kucenas, Bruce Appel, and Victor Ambros for critical comments and suggestions and Dr. Jeff Rohrbough and Dr. Ricardo Pineda for help with the FM1-43 experiments. We also thank Drs. Li-En Jao and Susan Wente for providing the *mxn1:TagRFP-T* fish.

Author Contributions

Conceived and designed the experiments: CW EJT JGP. Performed the experiments: CW EJT AFO DJC ALP AFM. Analyzed the data: CW EJT AFO BDC KB JGP. Contributed reagents/materials/analysis tools: CW EJT ALP. Wrote the paper: CW KB JGP.

References

- Sudhof TC, Rothman JE (2009) Membrane fusion: grappling with SNARE and SM proteins. *Science* 323: 474–477.
- Wickner W, Schekman R (2008) Membrane fusion. *Nat Struct Mol Biol* 15: 658–664.
- Jahn R, Scheller RH (2006) SNAREs—engines for membrane fusion. *Nat Rev Mol Cell Biol* 7: 631–643.
- Matteoli M, Pozzi D, Grumelli C, Condliffe SB, Frassoni C, et al. (2009) The synaptic split of SNAP-25: different roles in glutamatergic and GABAergic neurons? *Neuroscience* 158: 223–230.
- Choi UB, Strop P, Vrljic M, Chu S, Brunger AT, et al. (2010) Single-molecule FRET-derived model of the synaptotagmin 1-SNARE fusion complex. *Nat Struct Mol Biol* 17: 318–324.
- Vrljic M, Strop P, Ernst JA, Sutton RB, Chu S, et al. (2010) Molecular mechanism of the synaptotagmin-SNARE interaction in Ca²⁺-triggered vesicle fusion. *Nat Struct Mol Biol* 17: 325–331.
- Schiavo G, Stenbeck G, Rothman JE, Sollner TH (1997) Binding of the synaptic vesicle v-SNARE, synaptotagmin, to the plasma membrane t-SNARE, SNAP-25, can explain docked vesicles at neurotoxin-treated synapses. *Proc Natl Acad Sci U S A* 94: 997–1001.
- Blasi J, Chapman ER, Link E, Binz T, Yamasaki S, et al. (1993) Botulinum neurotoxin A selectively cleaves the synaptic protein SNAP-25. *Nature* 365: 160–163.
- Schiavo G, Santucci A, Dasgupta BR, Mehta PP, Jontes J, et al. (1993) Botulinum neurotoxins serotypes A and E cleave SNAP-25 at distinct COOH-terminal peptide bonds. *FEBS Lett* 335: 99–103.
- Smith R, Klein P, Koe-Schmitz Y, Waldvogel HJ, Faull RL, et al. (2007) Loss of SNAP-25 and rabphilin 3a in sensory-motor cortex in Huntington's disease. *J Neurochem* 103: 115–123.
- Dessi F, Colle MA, Hauw JJ, Duyckaerts C (1997) Accumulation of SNAP-25 immunoreactive material in axons of Alzheimer's disease. *Neuroreport* 8: 3685–3689.
- Ostenson CG, Gaisano H, Sheu L, Tibell A, Bartfai T (2006) Impaired gene and protein expression of exocytotic soluble N-ethylmaleimide attachment protein receptor complex proteins in pancreatic islets of type 2 diabetic patients. *Diabetes* 55: 435–440.
- Washbourne P, Thompson PM, Carta M, Costa ET, Mathews JR, et al. (2002) Genetic ablation of the t-SNARE SNAP-25 distinguishes mechanisms of neuroexocytosis. *Nature Neuroscience* 5: 19–26.
- Keller JE, Cai F, Neale EA (2004) Uptake of botulinum neurotoxin into cultured neurons. *Biochemistry* 43: 526–532.
- Sorensen JB, Nagy G, Varoqueaux F, Nehring R, Brose N, et al. (2003) Differential Control of the Releasable Vesicle Pools by SNAP-25 Splice Variants and SNAP-23. *Cell* 114: 75–86.
- Augustin I, Rosenmund C, Sudhof TC, Brose N (1999) Munc13-1 is essential for fusion competence of glutamatergic synaptic vesicles. *Nature* 400: 457–461.
- Gitler D, Takagishi Y, Feng J, Ren Y, Rodriguiz RM, et al. (2004) Different presynaptic roles of synapsins at excitatory and inhibitory synapses. *Journal of Neuroscience* 24: 11368–11380.
- Schoch S, Castillo PE, Jo T, Mukherjee K, Geppert M, et al. (2002) RIM1alpha forms a protein scaffold for regulating neurotransmitter release at the active zone. *Nature* 415: 321–326.
- Atouf F, Czernichow P, Scharfmann R (1997) Expression of neuronal traits in pancreatic beta cells. Implication of neuron-restrictive silencing factor/pressor element silencing transcription factor, a neuron-restrictive silencer. *J Biol Chem* 272: 1929–1934.
- Chong JA, Tapia-Ramirez J, Kim S, Toledo-Aral JJ, Zheng Y, et al. (1995) REST: a mammalian silencer protein that restricts sodium channel gene expression to neurons. *Cell* 80: 949–957.
- Wu J, Xie X (2006) Comparative sequence analysis reveals an intricate network among REST, CREB and miRNA in mediating neuronal gene expression. *Genome Biol* 7: R85.
- Vo NK, Cambronne XA, Goodman RH (2010) MicroRNA pathways in neural development and plasticity. *Curr Opin Neurobiol*.
- Qureshi IA, Mehler MF (2009) Regulation of non-coding RNA networks in the nervous system—what's the REST of the story? *Neurosci Lett* 466: 73–80.
- Schratt G (2009) microRNAs at the synapse. *Nat Rev Neurosci* 10: 842–849.
- Cohen JE, Lee PR, Chen S, Li W, Fields RD (2011) MicroRNA regulation of homeostatic synaptic plasticity. *Proc Natl Acad Sci U S A* 108: 11650–11655.
- Catterall WA, Few AP (2008) Calcium channel regulation and presynaptic plasticity. *Neuron* 59: 882–901.
- Verhage M, Sorensen JB (2008) Vesicle docking in regulated exocytosis. *Traffic* 9: 1414–1424.

28. Christodoulou F, Raible F, Tomer R, Simakov O, Trachana K, et al. (2010) Ancient animal microRNAs and the evolution of tissue identity. *Nature* 463: 1084–1088.
29. Kapsimali M, Kloosterman WP, de Bruijn E, Rosa F, Plasterk RH, et al. (2007) MicroRNAs show a wide diversity of expression profiles in the developing and mature central nervous system. *Genome Biol* 8: R173.
30. Wienholds E, Kloosterman WP, Miska E, Alvarez-Saavedra E, Berezikov E, et al. (2005) MicroRNA Expression in Zebrafish Embryonic Development. *Science* 309: 310–311.
31. Thatcher E, Flynt A, Li N, Patton J, Patton J (2007) MiRNA expression analysis during normal zebrafish development and following inhibition of the Hedgehog and Notch signaling pathways. *Dev Dyn* 236: 2172–2180.
32. Wei C, Salichos L, Wittgrove CM, Rokas A, Patton JG (2012) Transcriptome-wide analysis of small RNA expression in early zebrafish development. *RNA* 18: 915–929.
33. Risinger C, Salanek E, Soderberg C, Gates M, Postlethwait JH, et al. (1998) Cloning of two loci for synapse protein Snap25 in zebrafish: comparison of paralogous linkage groups suggests loss of one locus in the mammalian lineage. *J Neurosci Res* 54: 563–573.
34. Bark C, Bellingier FP, Kaushal A, Mathews JR, Partridge LD, et al. (2004) Developmentally regulated switch in alternatively spliced SNAP-25 isoforms alters facilitation of synaptic transmission. *Journal of Neuroscience* 24: 8796–8805.
35. Hepp R, Langley K (2001) SNAREs during development. *Cell Tissue Res* 305: 247–253.
36. Lu B (2003) BDNF and activity-dependent synaptic modulation. *Learn Mem* 10: 86–98.
37. Asakura T, Waga N, Ogura K, Goshima Y (2010) Genes required for cellular UNC-6/netrin localization in *Caenorhabditis elegans*. *Genetics* 185: 573–585.
38. Mai J, Fok L, Gao H, Zhang X, Poo MM (2009) Axon initiation and growth cone turning on bound protein gradients. *J Neurosci* 29: 7450–7458.
39. Cohen-Cory S, Kidane AH, Shirkey NJ, Marshak S (2010) Brain-derived neurotrophic factor and the development of structural neuronal connectivity. *Dev Neurobiol* 70: 271–288.
40. Lewis KE, Eisen JS (2003) From cells to circuits: development of the zebrafish spinal cord. *Prog Neurobiol* 69: 419–449.
41. Eisen JS (1991) Developmental neurobiology of the zebrafish. *J Neurosci* 11: 311–317.
42. Eisen JS, Myers PZ, Westerfield M (1986) Pathway selection by growth cones of identified motoneurons in live zebra fish embryos. *Nature* 320: 269–271.
43. Appel B, Kozh V, Glasgow E, Thor S, Edlund T, et al. (1995) Motoneuron fate specification revealed by patterned LIM homeobox gene expression in embryonic zebrafish. *Development* 121: 4117–4125.
44. Westerfield M, McMurray JV, Eisen JS (1986) Identified motoneurons and their innervation of axial muscles in the zebrafish. *J Neurosci* 6: 2267–2277.
45. Myers PZ, Eisen JS, Westerfield M (1986) Development and axonal outgrowth of identified motoneurons in the zebrafish. *J Neurosci* 6: 2278–2289.
46. Jao LE, Appel B, Wente SR (2012) A zebrafish model of lethal congenital contracture syndrome 1 reveals Glu1 function in spinal neural precursor survival and motor axon arborization. *Development* 139: 1316–1326.
47. Trevarrow B, Marks DL, Kimmel CB (1990) Organization of hindbrain segments in the zebrafish embryo. *Neuron* 4: 669–679.
48. Gaffield MA, Betz WJ (2006) Imaging synaptic vesicle exocytosis and endocytosis with FM dyes. *Nat Protoc* 1: 2916–2921.
49. Li W, Ono F, Brehm P (2003) Optical measurements of presynaptic release in mutant zebrafish lacking postsynaptic receptors. *J Neurosci* 23: 10467–10474.
50. Burgoyne RD, Morgan A (2003) Secretory granule exocytosis. *Physiol Rev* 83: 581–632.
51. Kammenberg K, Wittekindt NE, Tippmann S, Wolburg H, Ranke MB, et al. (2007) Mutant and Misfolded Human Growth Hormone is Rapidly Degraded Through the Proteasomal Degradation Pathway in a Cellular Model for Isolated Growth Hormone Deficiency Type II. *Journal of Neuroendocrinology* 19: 882–890.
52. Gray LJ, Dean B, Kronsbein HC, Robinson PJ, Scarr E (2010) Region and diagnosis-specific changes in synaptic proteins in schizophrenia and bipolar I disorder. *Psychiatry Res* 178: 374–380.
53. Kimura K, Mizoguchi A, Ide C (2003) Regulation of growth cone extension by SNARE proteins. *J Histochem Cytochem* 51: 429–433.
54. Osen-Sand A, Catsicas M, Staple JK, Jones KA, Ayala G, et al. (1993) Inhibition of axonal growth by SNAP-25 antisense oligonucleotides in vitro and in vivo. *Nature* 364: 445–448.
55. Osen-Sand A, Staple JK, Naldi E, Schiavo G, Rossetto O, et al. (1996) Common and distinct fusion proteins in axonal growth and transmitter release. *J Comp Neurol* 367: 222–234.
56. Igarashi M, Kozaki S, Terakawa S, Kawano S, Ide C, et al. (1996) Growth cone collapse and inhibition of neurite growth by Botulinum neurotoxin C1: a t-SNARE is involved in axonal growth. *J Cell Biol* 134: 205–215.
57. Igarashi M, Tagaya M, Komiya Y (1997) The soluble N-ethylmaleimide-sensitive factor attached protein receptor complex in growth cones: molecular aspects of the axon terminal development. *J Neurosci* 17: 1460–1470.
58. Zhou Q, Xiao J, Liu Y (2000) Participation of syntaxin 1A in membrane trafficking involving neurite elongation and membrane expansion. *J Neurosci Res* 61: 321–328.
59. Martínez-Arca S, Coco S, Mainguy G, Schenk U, Alberts P, et al. (2001) A common exocytic mechanism mediates axonal and dendritic outgrowth. *J Neurosci* 21: 3830–3838.
60. Grosse G, Grosse J, Tapp R, Kuchinke J, Gorsleben M, et al. (1999) SNAP-25 requirement for dendritic growth of hippocampal neurons. *J Neurosci Res* 56: 539–546.
61. Greenlee MH, Wilson MC, Sakaguchi DS (2002) Expression of SNAP-25 during mammalian retinal development: thinking outside the synapse. *Semin Cell Dev Biol* 13: 99–106.
62. Schiavo G, Matteoli M, Montecucco C (2000) Neurotoxins affecting neuroexocytosis. *Physiol Rev* 80: 717–766.
63. McKee AG, Loscher JS, O'Sullivan NC, Chadderton N, Palfi A, et al. (2010) AAV-mediated chronic over-expression of SNAP-25 in adult rat dorsal hippocampus impairs memory-associated synaptic plasticity. *J Neurochem* 112: 991–1004.
64. Tafoya LC, Shuttleworth CW, Yanagawa Y, Obata K, Wilson MC (2008) The role of the t-SNARE SNAP-25 in action potential-dependent calcium signaling and expression in GABAergic and glutamatergic neurons. *BMC Neuroscience* 9: 105.
65. Delgado-Martinez I, Nehring RB, Sorensen JB (2007) Differential abilities of SNAP-25 homologs to support neuronal function. *J Neurosci* 27: 9380–9391.
66. Bieker S, Schrott G (2008) microRNAs: tiny regulators of synapse function in development and disease. *J Cell Mol Med* 12: 1466–1476.
67. Ashraf SI, McLoon AL, Sclarsic SM, Kunes S (2006) Synaptic protein synthesis associated with memory is regulated by the RISC pathway in *Drosophila*. *Cell* 124: 191–205.
68. Baudry A, Mouillet-Richard S, Schneider B, Launay JM, Kellermann O (2010) miR-16 targets the serotonin transporter: a new facet for adaptive responses to antidepressants. *Science* 329: 1537–1541.
69. Kim J, Inoue K, Ishii J, Vanti WB, Voronov SV, et al. (2007) A MicroRNA feedback circuit in midbrain dopamine neurons. *Science* 317: 1220–1224.
70. Wayman GA, Davare M, Ando H, Fortin D, Varlamova O, et al. (2008) An activity-regulated microRNA controls dendritic plasticity by down-regulating p250GAP. *Proc Natl Acad Sci U S A* 105: 9093–9098.
71. Rajasethupathy P, Fiumara F, Sheridan R, Betel D, Puthanveetil SV, et al. (2009) Characterization of small RNAs in *Aplysia* reveals a role for miR-124 in constraining synaptic plasticity through CREB. *Neuron* 63: 803–817.
72. Simon DJ, Madison JM, Conery AL, Thompson-Peer KL, Soskis M, et al. (2008) The microRNA miR-1 regulates a MEF-2-dependent retrograde signal at neuromuscular junctions. *Cell* 133: 903–915.
73. Impey S, Davare M, Lasiek A, Fortin D, Ando H, et al. (2010) An activity-induced microRNA controls dendritic spine formation by regulating Rac1-PAK signaling. *Mol Cell Neurosci* 43: 146–156.
74. Parrish JZ, Xu P, Kim CC, Jan LY, Jan YN (2009) The microRNA bantam functions in epithelial cells to regulate scaling growth of dendrite arbors in *Drosophila* sensory neurons. *Neuron* 63: 788–802.
75. Tsurudome K, Tsang K, Liao EH, Ball R, Penney J, et al. (2010) The *Drosophila* miR-310 cluster negatively regulates synaptic strength at the neuromuscular junction. *Neuron* 68: 879–893.
76. Agostini M, Tucci P, Steinert JR, Shalom-Feuerstein R, Rouleau M, et al. (2011) microRNA-34a regulates neurite outgrowth, spinal morphology, and function. *Proc Natl Acad Sci U S A* 108: 21099–21104.
77. Schrott GM, Tuebing F, Nigh EA, Kane CG, Sabatini ME, et al. (2006) A brain-specific microRNA regulates dendritic spine development. *Nature* 439: 283–289.
78. Gao J, Wang WY, Mao YW, Graff J, Guan JS, et al. (2010) A novel pathway regulates memory and plasticity via SIRT1 and miR-134. *Nature* 466: 1105–1109.
79. Baudet ML, Zivraj KH, Abreu-Goodger C, Muldal A, Armisen J, et al. (2012) miR-124 acts through CoREST to control onset of *Sema3A* sensitivity in navigating retinal growth cones. *Nat Neurosci* 15: 29–38.
80. Doxakis E (2010) Post-transcriptional regulation of alpha-synuclein expression by mir-7 and mir-153. *J Biol Chem* 285: 12726–12734.
81. Lupp RA, Snider L, Weintraub H (1994) *Xenopus* embryos regulate the nuclear localization of XMyoD. *Genes and Development* 8: 1311–1323.
82. Sempere LF, Sokol NS, Dubrovsky EB, Berger EM, Ambros V (2003) Temporal regulation of microRNA expression in *Drosophila melanogaster* mediated by hormonal signals and broad-Complex gene activity. *Dev Biol* 259: 9–18.
83. Flynt A, Li N, Thatcher E, Solnica-Krezel L, Patton J (2007) Zebrafish miR-214 modulates Hedgehog signaling to specify muscle cell fate. *Nat Genet* 39: 259–263.
84. Tsuji M, Inanami O, Kuwabara M (2001) Induction of neurite outgrowth in PC12 cells by alpha -phenyl-N-tert-butylmethyluronium through activation of protein kinase C and the Ras-extracellular signal-regulated kinase pathway. *J Biol Chem* 276: 32779–32785.